Macromolecules

pubs.acs.org/Macromolecules Article

Generalized Model of Cooperative Covalent Polymerization: Connecting the Supramolecular Binding Interactions with the Catalytic Behavior

Hailin Fu,[§] Ryan Baumgartner,[§] Ziyuan Song,[§] Chongyi Chen, Jianjun Cheng,* and Yao Lin*

Cite This: *Macromolecules* 2022, 55, 2041−2050 Read Online

ACCESS | Metrics & More | Article Recommendations | Supporting Information

ABSTRACT: The dynamic assembly of actin and tubulin microfilaments from their subunits is imperative in enabling cell motility, cell division, and organismal muscle function. The nucleation-controlled growth kinetics that characterizes these protein polymerizations is facilitated by the cooperative and reversible noncovalent interactions of protein subunits. Although this growth kinetics has been realized in the supramolecular polymerization of numerous synthetic molecules, it is rare in covalent polymerizations since a cooperative binding event between a monomer and a polymer must also lead to catalysis of the polymerization. The ring-opening polymerization of *N*-carboxyanhydride monomers is one such system that has been shown to result in large degrees of cooperativity and self-acceleration depending on the polymer architecture. Herein, we apply recent experimental data to introduce a simple and generalized kinetic model of cooperative covalent polymerizations, incorporating a Michaelis−Menten-like equation into the rate laws to describe the binding of a monomer to the growing polymer chain explicitly. The treatment of the growing polymer chain as both a cooperative system and as a primitive "enzyme" with a distinct binding event not only increases the applicability of the model but also reduces the number of variables used to describe the system. The theoretical predictions are compared to experimental data with various levels of cooperativity. The application of this simple kinetic model across a broad range of macromolecular architectures with varying levels of cooperativity will help polymer chemists to discover similar mechanisms in nonpolypeptide systems and utilize them to create covalent analogues of natural cooperative systems. The model can be extended to cover a variety of cases in which additional intermediates or competitive reactants occur in the reaction pathway of cooperative covalent polymerization.

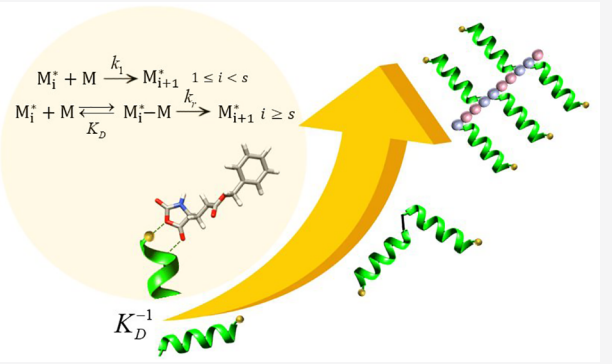

INTRODUCTION

Supramolecular interactions are leveraged by cells to catalyze chemical reactions essential for life including protein synthesis in ribosomes and the polymerization of cytoskeletal filaments.[1−8] These processes rely on a series of binding events and interactions that result in the structural changes of biomacromolecules to a more active state or the colocalization of biomolecules to vastly increase their local concentrations.[9,10] These cooperative supramolecular interactions act to greatly increase the rates of chemical reactions and have been utilized in a variety of synthetic polymerization processes, most often noncovalent,[11−22] but more recently in covalent systems.[23−26] One such covalent system identified early on by Doty and others is the synthesis of helical polypeptides such as poly(γ-benzyl-L-glutamate) (PBLG) via the ring-opening polymerization (ROP) of amino acid *N*-carboxyanhydrides (NCAs).[27−29] The reaction proceeds with a primary amine-based initiator to open the ring of the NCA monomer. Subsequent decarboxylation of the resulting structure results in the addition of a single amino acid to the growing polymer chain and the recovery of the active amine. In specific solvents, this polymerization was characterized by slow chain propagation, followed by a modest but distinct acceleration in a second stage that took place once α-helices could be stabilized in a solution [the degree of polymerization (DP) of 6−10].[27−29] Intrigued by the unusual cooperative behavior in this polymerization, we recently discovered that very strong cooperative effects can be induced in various macromolecular and supramolecular architectures that promote colocalization and polymer−monomer interactions to drastically accelerate the polymerization of NCAs into helical polypeptides.[23−26] Adapting the cooperative growth model for noncovalent systems (Figure 1a) first described by Oosawa[4,5] was successful

Received: December 22, 2021
Revised: February 4, 2022
Published: March 1, 2022

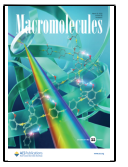

https://doi.org/10.1021/acs.macromol.1c02606
Macromolecules 2022, 55, 2041−2050

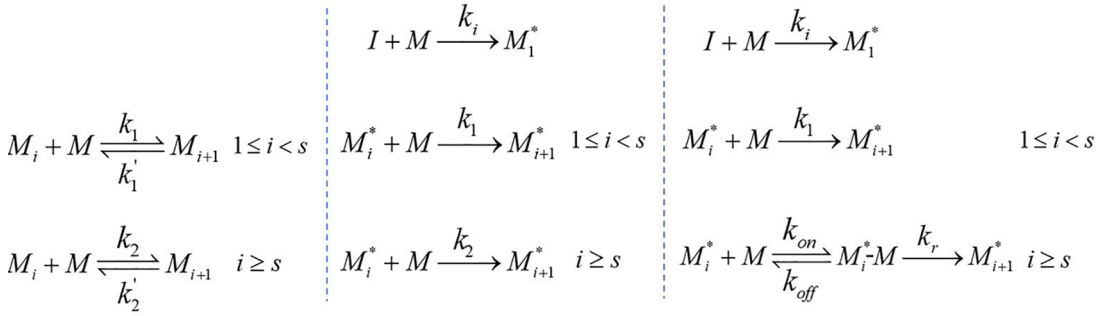

Figure 1. Key reaction processes involved in supramolecular cooperative polymerization and in covalent cooperative polymerization. (a) Cooperative supramolecular growth mechanism is represented by an ideal, Oosawa-type model that consists of two phases: first, monomers (M) slowly add into a linear chain of the DP of i (M_i), which, upon reaching a critical length (s, the nucleus size), rearranges into a helical chain and chain growth accelerates, e.g., due to more favorable interactions between the incoming monomer and the helical chain. k_1 and k_1' are the association and dissociation rate constants for the first (nucleation) stage, respectively; k_2 and k_2' are the rate constants for the second (propagation) stage. (b) Cooperative growth mechanism in supramolecular systems can be adapted to describe the two-staged, covalent cooperative polymerization found in the ROP-NCA of helical polypeptides by treating the addition of a monomer instead as an irreversible process and considering the chain initiation step (with a kinetic rate constant k_i) before the two successive growth stages. (c) With strong evidence of a reversible binding between incoming monomers and helical polymers in cooperative covalent polymerization, a chain growth mechanism with an incorporated adsorption step has been developed. In this model, the reaction occurs in two steps when the growing chain reaches the critical length s (e.g., folding into an α-helix). The monomer binds to the active chain to form the reaction complex ($M_i^* - M$), with an adsorption rate constant k_{on} and a desorption rate constant k_{off}. The subsequent attack of the active chain end on the bound monomer allows the chain elongation at a rate constant k_r. This two-stage, MM-type kinetic model reveals that cooperative covalent polymerization may be intrinsically catalytic in nature.

in modeling the two-stage kinetic profiles in the NCA-ROP (Figure 1b) across various polymer architectures.[23−25]

Recently, with nuclear magnetic resonance (NMR)-based experiments and molecular dynamics simulations, we elucidated that the auto-acceleration in NCA polymerizations is due to monomer binding to the actively growing N-terminus of α-helical polypeptides in the elongation stage (Figure 1c).[26] This mechanism is not unlike the classical Michaelis−Menten (MM)-type kinetics that describes enzymatic systems in which a distinct binding event of the substrate to the active site occurs.[30,31] Realizing that α-helical polypeptides may be treated as catalytic pseudo-species in the chain propagation reaction is important, as we can now examine across various macromolecular architectures by focusing on the factors that promote the "polymer−monomer" interactions to gain further insight into the widely different cooperative strengths observed in the auto-accelerated polymerization kinetics. Here, we consider this reversible binding event between the NCA monomers and the growing helical chains and introduce a generalized treatment of the cooperative covalent polymerization by approximating the rate laws for accelerated chain elongation explicitly using a MM-like equation. This approach reduces the number of parameters in the model and allows for potential extensions and modifications of the kinetic framework for autocatalytic polymerizations in general. The model can interpret the existing kinetic phenomena in ROP-NCAs obtained with various levels of cooperativity. The different cooperative strengths are simply quantified by the effective binding affinity in the model. The unified theoretical framework and experimental strategy presented here should accelerate the discovery of novel reaction systems that incorporate strong cooperative effects for the controlled synthesis of polymers.

THEORETICAL BASIS

Oosawa−MM Model of Cooperative Covalent Polymerization. Previously, we have shown that NCA monomers undergo reversible adsorption/desorption to the active polymerization site of the helical polypeptide prior to the irreversible ring-opening of the NCA monomer.[26] To describe this, a two-staged, Oosawa-type kinetic model was established with the monomer adsorption step incorporated into the elongation stage, as described by the successive reactions in Figure 1c, where M represents monomer and M_i^* denotes a polymer chain with a DP of i and an active site (*) at the end. In the initial stage of the chain growth where the DP of i is less than the critical chain length (s, the nucleus for helix formation), we treated the reaction between the monomer and the active end of the coil chain as a second-order reaction with a rate constant k_1. When $i \ge s$, the propagation rate increases due to cooperative interactions stemming from the formation of the α-helix. In this accelerated elongation stage, we considered the reaction to occur in two steps: first, the monomer binds to the active helical chain to form the reaction complex $M_i^* - M$, with an adsorption rate constant k_{on} and a desorption rate constant k_{off}; subsequently, the attack of the active end of the helical chain on the bound monomer triggers a ring-opening reaction and allows for the chain elongation with a rate constant k_r. Based on this model, it was then standard practice to write the concentration flux equations[26] (Figure S1) corresponding to the abovementioned scheme and determine their numerical solutions.

Although the concentration flux approach explicitly describes the microscopic processes of chain growth, the adsorption and desorption rate constants (k_{on} and k_{off}, respectively) cannot be individually determined with good accuracy, and usually it takes more iterations of numerical solutions to avoid local minima and find the best estimates of kinetic parameters from experimental data in comparison with the phenomenological model[23] shown in Figure 1b. Here, we describe a simple rate equation system by focusing on the time evolution of the principal moments: the mass concentration $m(t)$ (or the concentration of polymerized monomers) and the number concentration $P(t)$ of the polymers

https://doi.org/10.1021/acs.macromol.1c02606
Macromolecules 2022, 55, 2041−2050

$$m(t) = \sum_{i=s}^{\infty} iM_i(t), \qquad P(t) = \sum_{i=s}^{\infty} M_i(t)$$

and by incorporating the MM equation explicitly into the differential rate equations. Following the convention in cooperative supramolecular polymerization, we include in P any chains longer than the nucleus ($i \geq s$). The two quantities, $m(t)$ and $P(t)$, are experimentally most accessible, for example, by monitoring the monomer consumption in the reaction through spectroscopic methods. Their quotient $m(t)/P(t)$, gives the average length of the polymer DP, and can be verified by measuring the molecular weight (MW) of resulting polymers by gel permeation chromatography (GPC) or other standard methods.

The two-step reaction in the elongation stage is analogous to an enzymatic reaction described by MM-type kinetics in which the actively growing chain end acts as the "enzyme" and the monomer is the "substrate".[30,31] A reversible bimolecular binding occurs first between the growing chain and the monomer, followed by an irreversible unimolecular reaction that incorporates the bound monomer covalently into the chain and recovers the number of active chain ends. Under a quasi-steady-state assumption that generally holds for this type of catalytic polymerization, the rate equation of polymerized monomers can be described by the MM-type equation

$$\frac{dm(t)}{dt} = \frac{k_r M(t)P(t)}{K_D + M(t)} \tag{1}$$

where K_D is the equilibrium dissociation constant of monomers from the growing chain end ($K_D = k_{off}/k_{on}$), a catalytic pseudo-species acting like an enzyme in the MM mechanism. The differential equation describing the time evolution of monomer concentration $M(t)$ then follows

$$-\frac{dM(t)}{dt} = k_1 M(t)(I_0 - P(t)) + \frac{dm(t)}{dt} \tag{2}$$

where the first term is the rate of monomer consumption caused by the active chains being shorter than the critical length s, and I_0 is the concentration of initiators at time zero.

The kinetic equation for the number concentration of polymers $P(t)$ follows

$$\frac{dP(t)}{dt} = k_1 M_{s-1}(t)M(t) \tag{3}$$

where $M_{s-1}(t)$ represents the concentration of active chains (M^*_{s-1}) with the length of $s-1$ at time t and can be obtained by solving

$$\frac{dM_i(t)}{dt} = k_1 M(t)(M_{i-1}(t) - M_i(t)) \qquad 1 < i < s \tag{4}$$

$$\frac{dM_1(t)}{dt} = -k_1 M(t)M_1(t) \tag{5}$$

and we usually assume $M_1(0) = I_0$ for fast initiation reaction. Equations 1−5 establish the complete set of differential equations that incorporate the MM equation into the Oosawa−MM (OMM) model for numerical solutions.

In comparison with the model based on concentration flux equations, the fitting parameters of this model have now been reduced from five to four: s, k_1, k_r, and K_D. This allows for the determination of the unique set of fitting parameters by carrying out model-based analysis, even with a limited set of kinetic data. In addition, incorporating the MM-like equation into the rate equations allows for the potential extension and modification of the kinetic model for two-stage catalytic polymerizations in general. The MM equation holds for many mechanisms, even though the MM mechanism (e.g., $k_r \ll k_{off}$) is not always applicable.[32] The scheme can be extended to cover a variety of cases, for example, when k_r is comparable to k_{off} in a Briggs−Haldane-like kinetics, or when additional intermediates, either covalently or noncovalently bound, occur on the reaction pathway.[32,33] In most cases, the MM equation still applies, although K_D and k_r should be replaced by K_M and k_{cat}, which are combinations of various rate and equilibrium constants (e.g., $K_M = K_D + \frac{k_r}{k_{on}}$ in Briggs−Haldane kinetics). In this context, the rate equation for polymerized monomers can be generalized to

$$\frac{dm(t)}{dt} = \frac{k_{cat} M(t)P(t)}{K_M + M(t)} \tag{6}$$

while other rate equations remain the same. The adaptability of this generalized kinetic model is crucial for the discovery of new reaction systems that incorporate different or currently unknown cooperative behaviors into the growth of polymer chains. Major variables and parameters used in the OMM model are listed in Table 1 for quick reference.

Table 1. List of Symbols Used in the OMM Model of Cooperative Covalent Polymerization

symbol	property
s	critical chain length
k_i	initiation rate constant
k_1	second-order rate constant for the first (nucleation) stage of polymerization
K_D	dissociation constant of the noncovalently bound complex from the monomer and the growing chain end in the second (propagation) stage of polymerization
k_r	first-order rate constant of chain elongation reaction from the noncovalently bound complex
σ^{-1}	reciprocal of kinetic cooperativity factor, $\sigma^{-1} = k_r/(K_D k_1)$
I_0	initiator concentration
M_0	initial monomer concentration
K_M	apparent dissociation constant of the Michaelis complex, K_D is replaced by K_M in the generalized OMM model to hold for complex reaction mechanisms
k_{cat}	apparent first-order rate constant for the chemical conversion from the Michaelis complex, k_r is replaced by k_{cat} in the generalized OMM model to hold for complex reaction mechanisms

Binding Equilibrium Facilitates a Saturation Effect on the Chain Growth Kinetics. In cooperative supramolecular polymerization, the kinetic cooperativity factor (σ) is defined as $\sigma^{-1} = k_2/k_1$ (Figure 1a), where a large value of σ^{-1} implies a higher cooperativity and $\sigma^{-1} = 1$ implies no cooperativity. Similarly, the kinetic cooperativity factor for OMM-type cooperative covalent polymerization can be approximately defined as $\sigma^{-1} = k_r/(K_D k_1)$. For a system with a defined critical chain length, s, the shape of polymerization kinetics is mainly controlled by the cooperativity factor and the initial monomer−initiator ratio (M_0/I_0). Solving the differential eqs 1−5 numerically for different σ^{-1} and M_0/I_0 yields the various kinetic curves shown in Figure 2a,b, where the fraction of polymerized monomers is plotted against dimensionless time $\tau = tk_1M_0$. It is not surprising that an enzyme-like saturation effect against increasing σ^{-1} is clearly evidenced in the

https://doi.org/10.1021/acs.macromol.1c02606
Macromolecules 2022, 55, 2041−2050

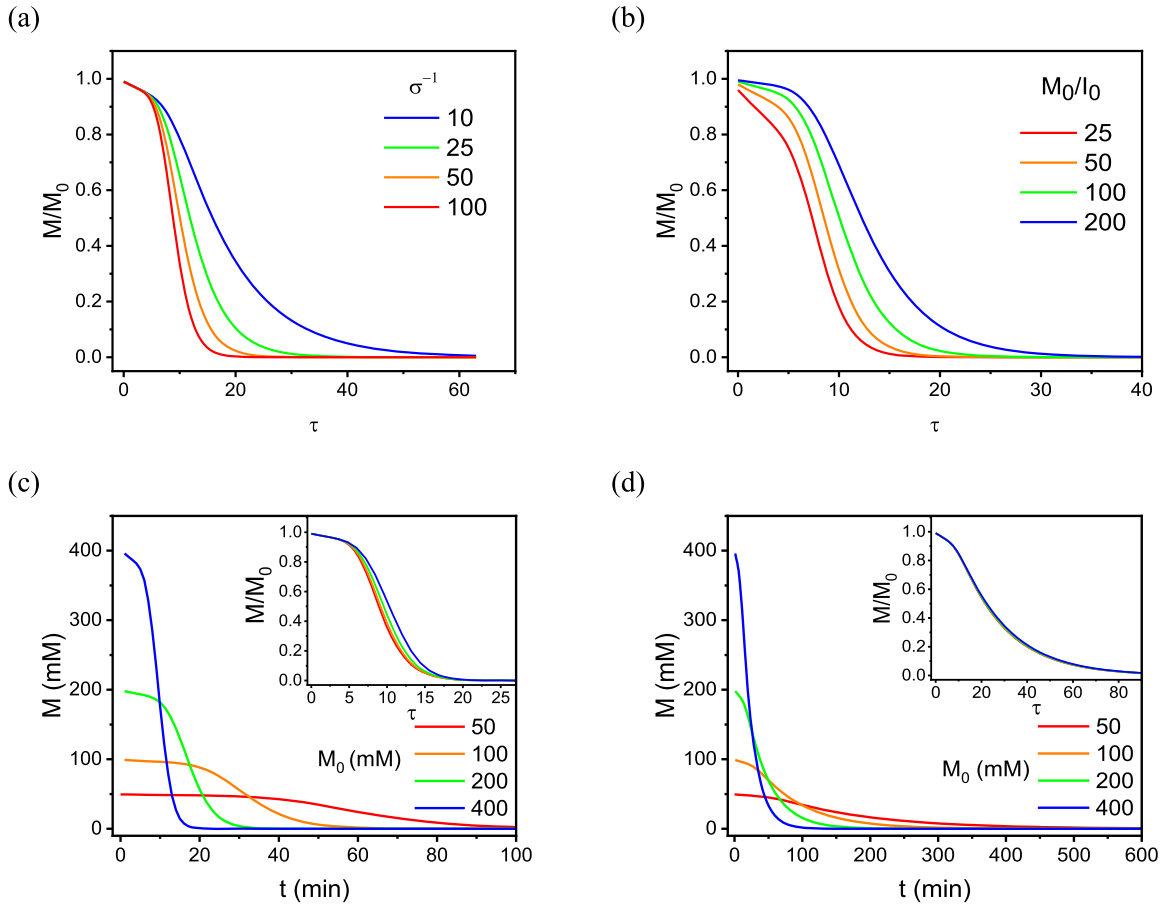

Figure 2. Simulations with the OMM model of cooperative covalent polymerization. (a,b) Plots of the fraction of the monomer versus rescale time ($\tau = tk_1M_0$) for test cases with $s = 10$, $k_1 = 0.05\ M^{-1}\ s^{-1}$, $k_r = 1\ s^{-1}$, and $M_0/I_0 = 100$, at selected values of σ^{-1} (a), and $s = 10$, $k_1 = 0.05\ M^{-1}\ s^{-1}$, $k_r = 1\ s^{-1}$, and $\sigma^{-1} = 50$, at selected values of M_0/I_0 (b). The shape of the curve is heavily influenced by σ^{-1} and the M_0/I_0 ratio. (c) Plots of the monomer concentration vs time for test cases with $s = 10$, $k_1 = 0.05\ M^{-1}\ s^{-1}$, $k_r = 1\ s^{-1}$, $K_D = 0.25$ M, and $M_0/I_0 = 100$, at selected values of M_0. The inset shows the plot of the fraction of the monomer vs rescale time for the same condition. (d) Same as (c), but $K_D = 4$ M. The difference in K_D changes σ^{-1} from 80 in (c) to 5 in (d). The inset shows that the concentration dependence of kinetic profiles in the dimensionless form almost vanishes.

accelerated propagation stage. In addition, binding equilibrium between monomers and the growing helical chains introduces the terms that explicitly depend on M_0 in the differential equations (see the equations in dimensionless form in Figure S2). Figure 2c shows the predicted kinetic curves from solving eqs 1−5 numerically for an identical set of s, rate and equilibrium constants, and M_0/I_0, but with different M_0. Increasing M_0 changes the shape of the kinetic profile even in the dimensionless form (inset of Figure 2c), which contrasts with the prediction of the earlier phenomenological model.[23] The dependence on the monomer concentration reaches saturation when M_0 is far above K_D. Figure S3a shows how the DP of the resulting polymers compares with M_0/I_0 (DP*) based on the kinetic curves in Figure 2c. In the limit that σ^{-1} tends to 1, the concentration dependence of kinetic profiles vanishes and DP/DP* tends to 1 (Figures 2d and S3b), where eventually single-stage kinetics are recovered. The substantial dependence of kinetic curves and DPs on M_0 is a characteristic of the OMM kinetic model and is clearly evidenced in the experiments.

This exercise also indicates that the elucidation of the catalytic nature of cooperative covalent polymerizations often requires a "global" analysis of the kinetic profiles collected from a series of experiments with different M_0. This has become a routine practice in the study of supramolecular polymerization; however, it is usually not carried out in covalent polymerization. Besides, a good choice of M_0 range (to span the saturating region) is important to obtain a reliable outcome from the model-based analysis. At concentrations far above the saturation concentration, K_D cannot be determined. At concentrations much lower than the saturation concentration, the accuracy in determining K_D is relatively poor. In the next section, we demonstrate the analysis of two-stage kinetic profiles from the ROP-NCA of helical polypeptides under different cooperative strengths. We show that the generalized OMM model can correctly account for the course of monomer consumption over time as observed in the experimental data, and the corresponding trend of the average DP of the polymers.

RESULTS AND DISCUSSION

Experimental Setup of ROP-NCA Kinetics and Polypeptide Characterization. Currently, many experimental studies on cooperative covalent polymerization are based on the polymerization of the γ-benzyl-L-glutamate NCA (BLG-NCA), mainly due to the facile synthesis and purification, the excellent solubility of the monomer and the resulting polypeptide, PBLG (Scheme 1a), and the characteristic coil-

https://doi.org/10.1021/acs.macromol.1c02606
Macromolecules 2022, 55, 2041−2050

Scheme 1. ROP of NCA with Different Initiating Systems[a]

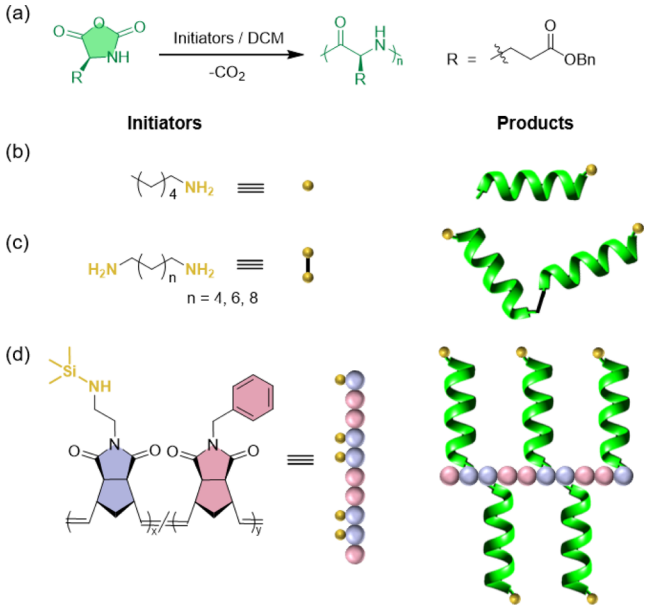

[a](a) Chemical structures of BLG-NCA monomers and PBLG polypeptides. (b–d) Chemical structures of the (macro)initiators and schematic illustration of the corresponding polypeptides grown from the (macro)initiators. Three initiating systems with increasing density of initiating sites were evaluated: a homopolymerization system initiated by *n*-hexylamine (b), a "hinged" polymerization system initiated by diaminoalkane (c), and a brush-like polymerization system initiated by a poly(NB) bearing pendant trimethylsilylamino side chains (d).

to-helix transition during the polymerization.[23] The polymerization kinetics used in this study and the MW distribution (MWD) profiles of the resulting polymers were obtained from our previous published work and new experiments (see the Supporting Information).[23,24,26] Briefly, Fourier transform infrared spectroscopy or proton NMR spectroscopy were used to monitor the disappearance of signals from NCA monomers, which, after normalization, indicated the extent of polymerization in a quantitative manner. Specifically, the polymerization kinetics of three different initiating systems were collected, with increasing density of initiating sites: a low-cooperativity system using *n*-hexylamine as the initiator (Scheme 1b), a medium-cooperativity system initiated from three diaminoalkane (1,6-diaminohexane, 1,8-diaminooctane, and 1,10-diaminodecane, named as C_6-diNH_2, C_8-diNH_2, and C_{10}-diNH_2, respectively, in Scheme 1c), and a high-cooperativity system with poly(norbornene) [poly(NB)] bearing pendant trimethylsilylamino side chains as the brush-like macroinitiator (Scheme 1d).

Polymerization of Helical Homopolypeptides at Low Cooperative Strength. We first used the new generalized OMM model to analyze the linear, self-catalyzed polymerization of BLG-NCAs initiated by primary amines into helical PBLG in dichloromethane (DCM). This two-stage, auto-accelerated polymerization in solvents of low dielectric constant proceeds with reversible NCA binding and the subsequent irreversible ring-opening reaction of the NCA monomer. The 27 kinetic profiles collected from three initial monomer concentrations, each with three different M_0/I_0 ratios, and three replicates per condition,[26] were fitted by solving the differential rate eqs 1–5 numerically (Figure 3a–c). A global fit was obtained for 27 sets of kinetic data by sharing the same s and k_r (s = 10 and k_r = 0.4 s^{-1}), while allowing k_1 and K_D to be optimized for 9 individual conditions. The MWs predicted by the kinetic model based on the optimized parameters are in good agreement with the GPC results from the polymers (Table S1). Figure 3d indicates an interesting correlation between k_1 and K_D with I_0 (the concentration of active chains), even though the difference in k_1 is rather small. In the nucleation stage (k_1), the presence of short, coil-like chains in which NCA monomers can undergo nonproductive binding with amide groups may interfere with desired binding at the N-terminus. The effect is more pronounced with fewer chains in the solution and may cause the modest decrease of k_1 with lower I_0. The effect, however, should not play an important role during the fast propagation stage, as the formation of helices with an intrachain H-bonding network prevents NCAs from binding nonspecifically. It is known that the increasing concentration of PBLGs in DCM or chloroform may facilitate some bundling of the helices in the solution, which explains the increase of binding equilibrium constants with I_0 due to a higher "effective concentration" of initiator sites. The effect is more clearly revealed in the polymerization of hinged polypeptide systems (vide infra), in which two growing chains are covalently connected by a synthetic linker.

Polymerization of "Hinged" Polypeptides at Medium Cooperative Strength. When linear aliphatic diamines are used as initiators for the synthesis of helical polypeptides, the polymerization leads to the formation of "hinged" polypeptides in which two chains are grown connected through the flexible diamine initiator. The reaction again follows a two-stage, nucleation-controlled polymerization kinetics, with the acceleration more than 30-fold faster than that in the polymerization of a single isolated polypeptide chain.[24] Having two growing helical chains connected by a linker affects the binding interactions between monomers and the active ends, due to the effect of "local" concentration. We examined the polymerization initiated by three different linkers with various spacer lengths (C_6-diNH_2, C_8-diNH_2, and C_{10}-diNH_2), each at three different M_0 (0.05, 0.10, and 0.15 M, respectively), while keeping M_0/I_0 identical. By sharing the same k_r and s globally, the same K_D for each type of linker, but allowing k_1 to be individually optimized, a global fit was obtained for nine sets of kinetic data with varying M_0 and I_0 (Figure 4a–c). Such as in the polymerization of homo-PBLG, k_1 increases slightly with I_0 for the same spacer (Figure 4d). K_D is independent of I_0 but is a function of the length of the spacer. The MWs predicted by the kinetic model based on the optimized parameters are in good agreement with the GPC results from the polymers as well (Table S2 and Figure S4). By linking two active growing sites in the proximity, the effective binding affinity of NCA to the helical chains increases by 20–50 fold, depending on the diamine spacer length. The increase in the effective binding coefficient may arise from two effects. The first effect is due to the higher local concentration of initiating sites (Mi^*) and the second is due to the higher local concentration of the NCA monomer (M). The first effect stems from the diamine linker, which brings initiating sites into proximity to one another. The second is due to the colocalization of monomers, as monomers bound to one helix may react with the active end of the other helix in the same macromolecules. Proximity and colocalization are powerful forces used in biology to accelerate reactions, for instance, in protein allostery.[9] This effect of colocalization on

https://doi.org/10.1021/acs.macromol.1c02606
Macromolecules 2022, 55, 2041–2050

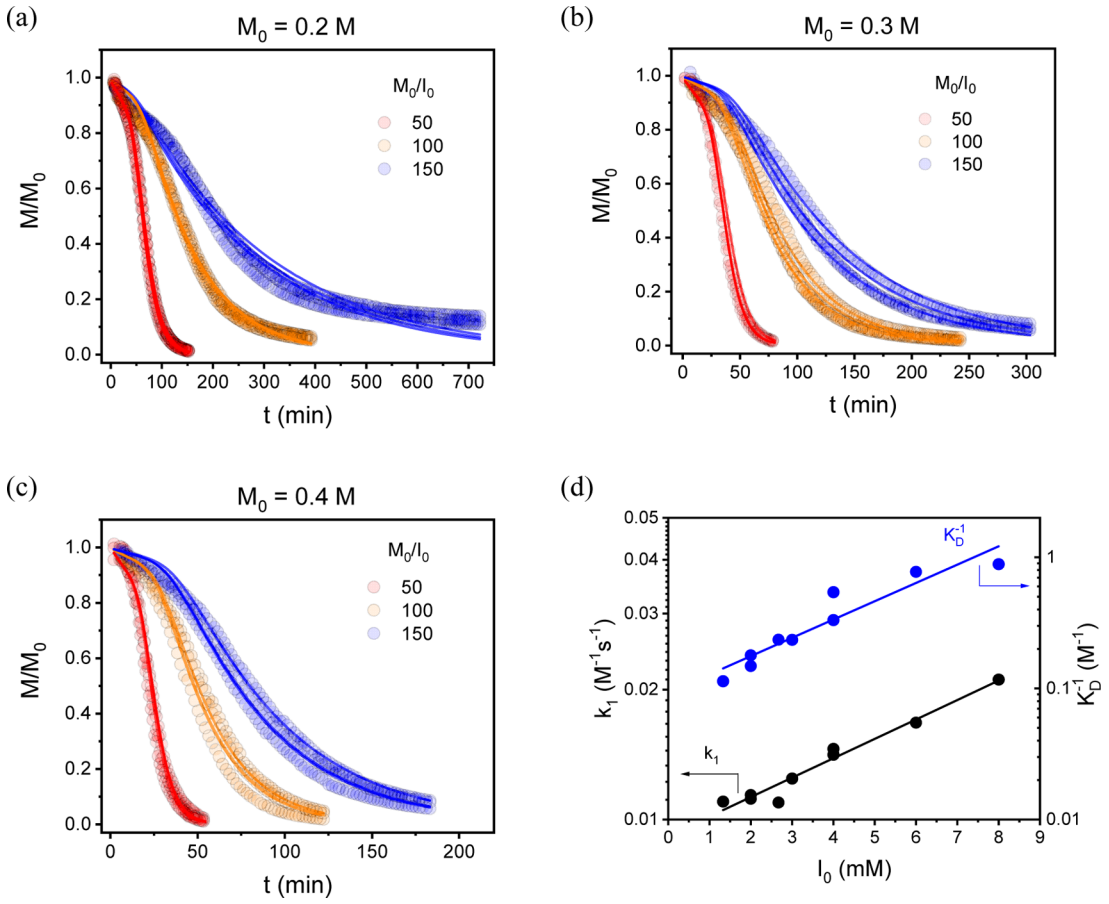

Figure 3. Analysis of self-catalyzed polymerization of helical polypeptides with the OMM model. (a–c) Polymerization kinetics of BLG-NCA in DCM was initiated by hexylamine with M_0 = 0.2 (a), 0.3 (b), and 0.4 M (c). Three M_0/I_0 ratios (50, 100, and 150) were tested for each M_0, each with three replicates. The kinetic data (circles) is fit with the OMM model (solid lines) by sharing the same s and k_r (s = 10 and k_r = 0.4 s^{-1}) for all the 27 profiles, while allowing k_1 and K_D to be optimized for 9 individual conditions. (d) Extracted rate constants for the nucleation stage (k_1) and the association equilibrium constant (K_D^{-1}) from (a–c). The results show an increase of k_1 and K_D^{-1} with increasing initiator concentration I_0, possibly due to the existence of some segregation of polymers in the solution.

effective binding is large and is also evidenced in the first stage of polymer growth, as k_1 shows a similar dependence on the spacer length (Figure 4d). This suggests that the proximity of two active chains can also enhance the interaction of NCA with the shorter chains in their coil state. In practice, however, it is difficult to separate the adsorption term explicitly from the rate constant in the nucleation stage, and it is also unnecessary, as k_1 can be determined with high accuracy from the kinetic profiles. Again, the OMM model functions very well to predict the kinetic profiles of cooperative systems of moderate strength.

Polymerization of Brush-Like Polypeptides at Strong Cooperative Strength. One of the fastest self-acceleration of NCA polymerizations was found in a brush-like polymer system that consists of a linear poly(NB) scaffold containing a high density of initiating groups from which polypeptide chains are grown.[23] NCAs condense on to the initiation sites along the polymeric scaffold to form polypeptide chains, which fold into α-helices upon reaching a critical chain length ($s \sim 10$). The rate of acceleration was drastic (up to 1000-fold), and was shown to be regulated according to the grafting density (f) of initiators on the polymeric backbone of a random copolymer of NB and inactive spacer groups (Figure 5a). By assuming $k_1 = k_1^0 \times f$ and $K_D^{-1} = K_D^{0-1} \times f$, the optimized fits shown in Figure 5a, all based on an identical set of rate and equilibrium constants (s = 10, k_1^0 = 0.12 M^{-1} s^{-1}, K_D^0= 0.026 M, and k_r = 1 s^{-1}), demonstrate an excellent agreement between the model prediction and the experimental results with polymeric initiators of four different chain grafting densities. In the densely packed, brush-like macromolecular architecture, both the rebinding and the colocalization effects are maximized to facilitate a significantly increased local molarity between NCA and active chain ends. Varying the grafting density provides a direct means to regulate the kinetics by controlling the extent of colocalization of active chains. This again suggests that the strong auto-acceleration behavior is mainly due to the enhanced binding interaction between NCA monomers and the high density of actively growing chains in the brush. Figure 5b shows the model-predicted MWDs based on the estimated rate constants and their comparison with the GPC measurements (insets of Figure 5b and Table S3). Except for the highest grafting density, the model agrees very well with the experiments. In contrast, if we do not consider the binding step explicitly in the propagation stage and use the phenomenological model[23] used in the original paper, although the kinetic profiles can be fitted individually, the model would predict MWs that significantly deviate from the GPC results (Figure S5). The result show that a vast enhancement of the polymerization rate can be induced by facilitating supra-

https://doi.org/10.1021/acs.macromol.1c02606
Macromolecules 2022, 55, 2041−2050

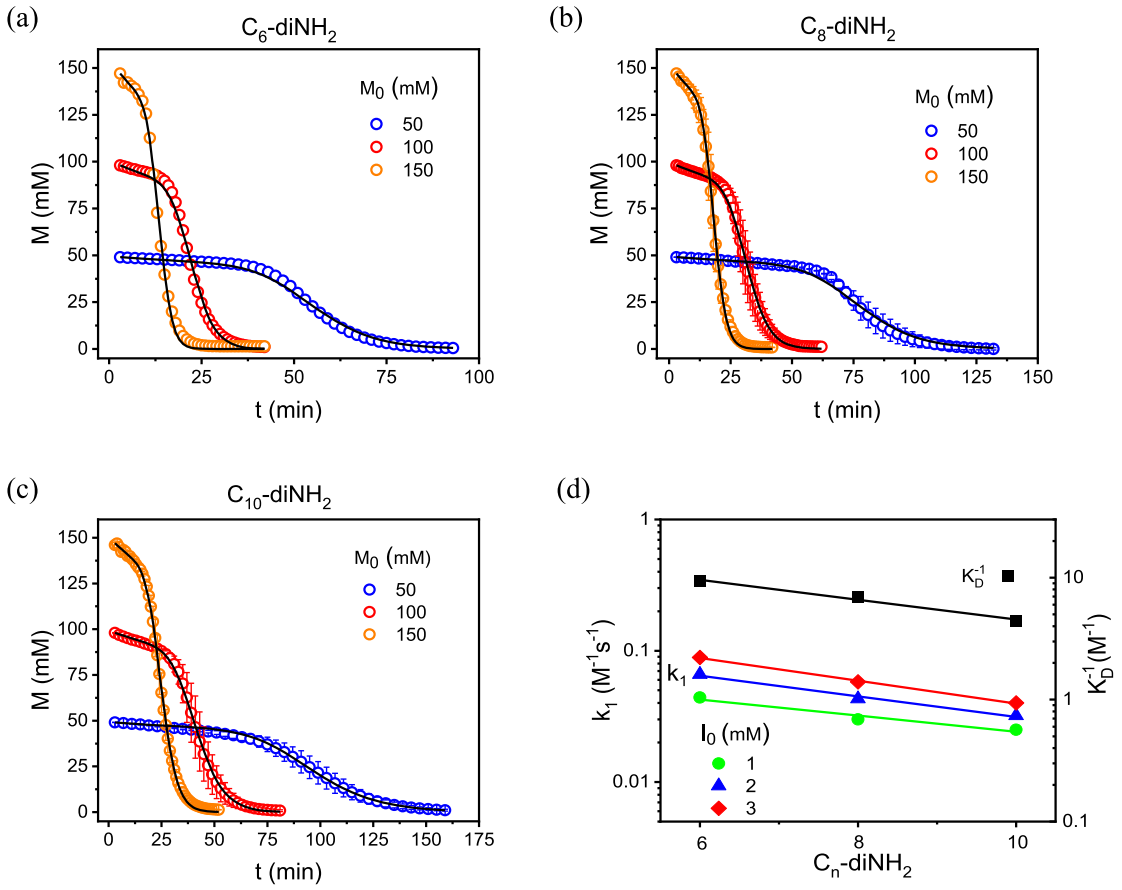

Figure 4. Analysis of polymerization of "hinged" helical polypeptides with the OMM model. (a–c). Kinetic data (circles) obtained from the polymerization of BLG-NCA in DCM using 1,6-diaminohexane (C_6-diNH$_2$) (a), 1,8-diaminooctane (C_8-diNH$_2$) (b), and 1,10-diaminodecane (C_{10}-diNH$_2$) (c) as the initiator at M_0/I_0 = 50, and at selected value of M_0 = 50, 100, or 150 mM, respectively. Error bars represent standard deviations from three independent measurements at each condition. The nine sets of kinetic data are fit with the OMM model by sharing the same s and k_r globally (s = 10 and k_r = 1 s^{-1}) and the same K_D for each type of initiator, but allowing k_1 to be individually optimized. (d) Extracted k_1 and K_D^{-1} from (a–c) for different C_n-diNH$_2$. The results show the dependence of the effective binding affinity of NCA to the helical chains on the spacer length, resulting from the proximity and colocalization of two active chains from the diamine initiators.

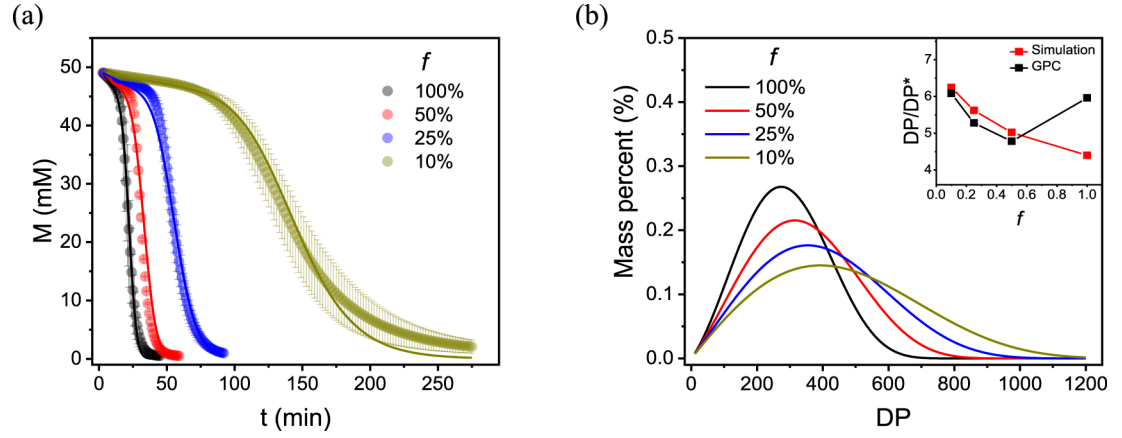

Figure 5. Analysis of "brush" polymerization of helical polypeptides with the OMM model. (a) Kinetic data (circles) obtained from the polymerization of BLG-NCA with random copolymer macroinitiators (M_0/I_0 = 50) of varying densities of the initiating group (f = 10, 25, 50, and 100%) is fit with the OMM model (solid lines) globally at s = 10, k_1^0 = 0.12 M^{-1} s^{-1}, K_D^0 = 0.026 M, and k_r = 1 s^{-1}. (b) Predicted MWD profiles based on the kinetic profiles in (a). Calculated DP (in red squares) at various f is compared to the GPC results (in black squares) in the inset. DP* = M_0/I_0 is used for normalization.

molecular interactions of reaction partners in a predefined macromolecular architecture.

From single helices to "hinged" double helices and an array of helices attached on a polymeric backbone, the OMM model successfully described the kinetics of the ROP-NCA reactions with an almost identical k_r and a K_D that is varied by two to three magnitudes across different macromolecular structures. The difference in k_1 may also be accounted for by a similar

https://doi.org/10.1021/acs.macromol.1c02606
Macromolecules 2022, 55, 2041–2050

binding interaction between the monomer and active chains in the first growing stage. Altogether, the data suggests that the local enrichment of growing chains accomplished by the macromolecular structures and the enhanced monomer adsorption facilitated by the neighboring binding sites has a profound effect on the effective binding strength of the growing chains and ultimately the catalytic nature of auto-accelerated, cooperative covalent polymerizations (Scheme 2).

Scheme 2. Summary of Structural Effect on the Enhanced Binding

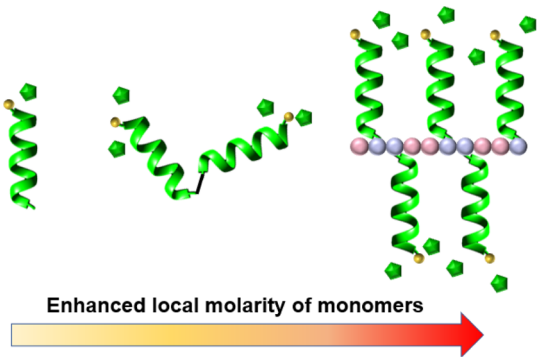

Applicability of the Model for the Complex Reaction Mechanism. Although the cooperative covalent polymerization described here can be summarized using relatively simple equations, other systems may present additional complexity. For example, it is not unusual that additional intermediates, covalent or noncovalent, occur in the reaction pathway of actual chemical reactions, as schematically shown in Figure 6a. To test whether the generalized OMM model still holds for this complex mechanism, we first established the corresponding concentration flux equations (Figure S6) from the reaction scheme and simulated the kinetic profiles of polymerization by the numerical method (Figure 6b). Then, we examined whether the complete set of kinetic profiles (e.g., starting from different M_0) can still be described by the generalized OMM model (eqs 2−6), in which K_D and k_r are now replaced by K_M and k_{cat}. We found that, in most cases, the generalized OMM model is a good approximation for the cooperative covalent polymerization with hypothesized multiple intermediates, resulting in unique K_M and k_{cat} from the fitting (Figure 6b, solid lines). We note that K_M and k_{cat} are now combinations of various rate and equilibrium constants and cannot be assigned to a particular molecular process. An analogue to the MM parameters commonly used in enzymatic reactions, K_M should be regarded as an apparent dissociation constant, and k_{cat} as the apparent first order rate constant for the chemical conversion. Figure 6c shows how the fitted K_M and k_{cat} are related with K_D and k_r used in the simulation of kinetic profiles, respectively, when the equilibrium constant for forming the second intermediate ($K' = k_+/k_-$) varies by a few orders in magnitude. By applying the steady-state assumption to the intermediates, the apparent propagation rate constant in the second stage can be derived and compared with the form of the MM equation, resulting in a simple analytic equation of K_M and k_{cat} as

$$K_M = \frac{k_+k_r + k_{off}(k_- + k_r)}{k_{on}(k_+ + k_- + k_r)} \approx \frac{K_D}{1 + K'}$$

$$k_{cat} = \frac{k_+k_r}{k_+ + k_- + k_r} \approx \frac{k_r}{1 + 1/K'}$$

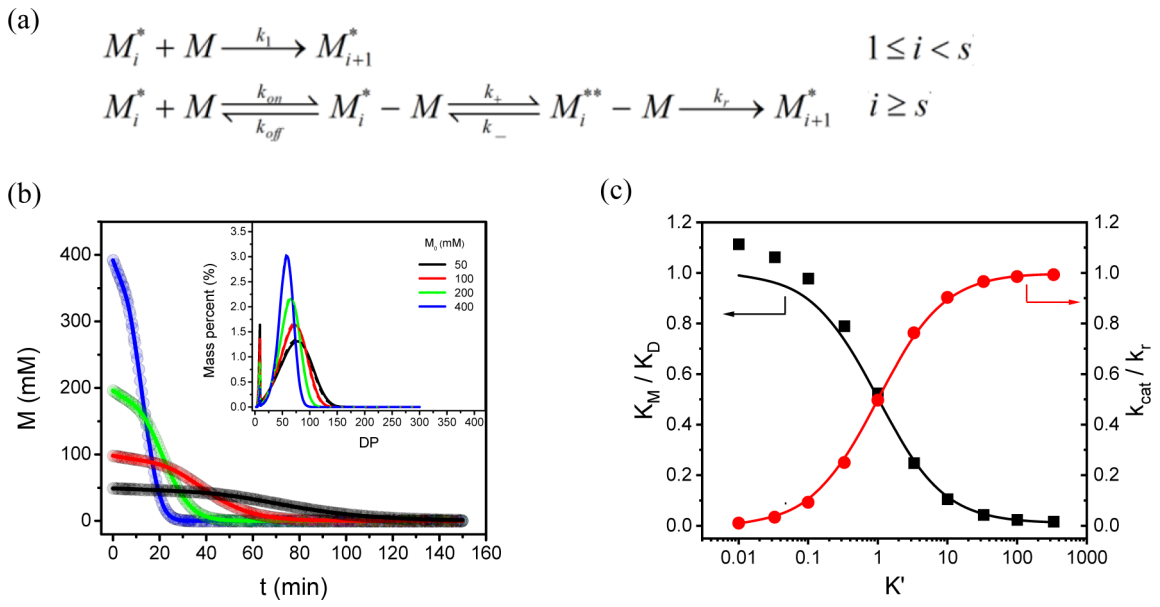

Figure 6. Validating the applicability of the OMM model for the complex reaction mechanism. (a) Reaction scheme for a case in which an additional intermediate occurs in the accelerating stage of cooperative covalent polymerization, k_+/k_- being the equilibrium constant (K') for forming the second intermediate. (b) Plots of the monomer concentration (in circles) vs time for test cases with $s = 10$, $M_0/I_0 = 50$, $k_1 = 0.05$ M^{-1} s^{-1}, $k_{on} = 1 \times 10^3$ M^{-1} s^{-1}, $k_{off} = 1 \times 10^2$ s^{-1}, $k_r = 1$ s^{-1}, $k_+ = 1 \times 10^3$ s^{-1}, and $k_- = 1 \times 10^4$ s^{-1}, at selected values of M_0. The kinetic profiles simulated can be globally fit by the generalized OMM model (solid lines) based on an identical set of parameters ($s = 10$, $k_1 = 0.05$ M^{-1} s^{-1}, $K_M = 0.1$ M, and $k_{cat} = 0.09$ s^{-1}). Inset: predicted MWD profiles based on the obtained parameters (dash lines) match well with the original MWD profiles (solid lines). (c) Dependence of K_M and k_{cat} on K', obtained from fitting the simulated kinetic profiles of (a) by the generalized OMM model.

https://doi.org/10.1021/acs.macromol.1c02606
Macromolecules 2022, 55, 2041−2050

when k_r is relatively small. The solid lines in Figure 6c show the prediction from the equations, in good agreement with the fitting results obtained numerically at individual values of K'.

We provide another example in which the generalized OMM model can accurately describe the covalent cooperative polymerization in which a competitive side reaction occurs in the accelerating stage (Supporting Information and Figures S7, S8). As in the polymerization reaction, it is common for a substrate molecule in the solution to bind in an alternative unreactive mode at the active site of the growing chain. The occurrence of such a competitive inhibition on the reaction pathway can be examined in a similar way to that for multiple intermediates. Again, the MM-like parameters in the OMM model can be uniquely obtained from the kinetic profiles and approximated by a simple analytic function of rate and equilibrium constants, as long as the competitive inhibition is not dominating the reaction. Reactions with even higher complexity can be treated by combining the multiple intermediates with the multiple competitive pathways.

The generalized OMM model should therefore provide a practical solution to predict the overall kinetic behavior and the MWD of resulting polymers and offer insightful information on the reaction mechanism. It remains to be seen to what extent the kinetic phenomena in novel systems other than the ROP-NCA obey the generalized OMM model, for all intents and purposes. It is reasonable to expect that, as the MM equation holds for many enzymatic and catalytic reactions, the OMM model should interpretate a variety of cooperative covalent polymerizations in which noncovalent interactions interplay with covalent interactions. The prototype enzymatic behavior found in the auto-accelerated polymerization of helical polypeptides in varying macromolecular architectures is likely not a coincidence, but due to the catalytic nature of cooperative covalent polymerization in general and the essential role of supramolecular binding interaction in this type of polymerization reactions.

CONCLUSIONS

The successful combination of the classical models of Oosawa and MM has shown that artificial polymer systems can be created in the likeness of complex biological systems. In this work, we successfully modeled and demonstrated that a synthetic polypeptide can behave as an "enzyme" by reversibly binding and catalyzing a chemical reaction. In this case, however, the polypeptide enzyme acts to catalyze a chemical reaction that results in its own growth without any need for specific amino acid side chains. Instead, this polymerization relies on the structural features of the α-helix to bind and catalyze the polymerization, and the effect can be amplified by increasing the local molarity of growing chains in the proximity. This remarkable feature is so far unique to the ROP, however, the model used to describe it can be leveraged to identify other polymerizations with cooperative elements and added complexity.

ASSOCIATED CONTENT

Supporting Information

The Supporting Information is available free of charge at https://pubs.acs.org/doi/10.1021/acs.macromol.1c02606.

Materials; instruments and characterization methods; experimental methods for polymerization kinetics; GPC characterization of resulting polypeptides; methods for kinetic modeling; description of the cooperative covalent polymerization model with a competitive side reaction; concentration flux kinetic equations; dimensionless form of the kinetic equations; analysis of the DPs of the resulting polymers; GPC light scattering traces for "hinged" polypeptides; simulation results for the cooperative covalent model with an inhibitive, competing side reaction; and detailed fitting results for homopolypeptides, "hinged" polypeptides, and "brush" polypeptides, and comparison with GPC analysis (PDF)

AUTHOR INFORMATION

Corresponding Authors

Jianjun Cheng − *Department of Materials Science and Engineering and Department of Chemistry, University of Illinois at Urbana-Champaign, Urbana, Illinois 61801, United States;* orcid.org/0000-0003-2561-9291; Email: jianjunc@illinois.edu

Yao Lin − *Department of Chemistry and Polymer Program at the Institute of Materials Science, University of Connecticut, Storrs, Connecticut 06269, United States;* orcid.org/0000-0001-5227-2663; Email: yao.lin@uconn.edu

Authors

Hailin Fu − *Department of Chemistry and Polymer Program at the Institute of Materials Science, University of Connecticut, Storrs, Connecticut 06269, United States;* orcid.org/0000-0002-3972-7659

Ryan Baumgartner − *Department of Materials Science and Engineering and Department of Chemistry, University of Illinois at Urbana-Champaign, Urbana, Illinois 61801, United States*

Ziyuan Song − *Department of Materials Science and Engineering and Department of Chemistry, University of Illinois at Urbana-Champaign, Urbana, Illinois 61801, United States;* orcid.org/0000-0002-3165-3712

Chongyi Chen − *Department of Materials Science and Engineering and Department of Chemistry, University of Illinois at Urbana-Champaign, Urbana, Illinois 61801, United States*

Complete contact information is available at: https://pubs.acs.org/10.1021/acs.macromol.1c02606

Author Contributions

[§]H.F., R.B., and Z.S. contributed equally.

Notes

The authors declare no competing financial interest.

ACKNOWLEDGMENTS

This work was supported by the NSF grant (DMR 1809497 to Y.L. and CHE-1709820 to J.C.).

REFERENCES

(1) Ramakrishnan, V. Ribosome structure and the mechanism of translation. *Cell* **2002**, *108*, 557−572.

(2) Sievers, A.; Beringer, M.; Rodnina, M. V.; Wolfenden, R. The ribosome as an entropy trap. *Proc. Natl. Acad. Sci. U.S.A.* **2004**, *101*, 7897−7901.

(3) Schmeing, T. M.; Ramakrishnan, V. What recent ribosome structures have revealed about the mechanism of translation. *Nature* **2009**, *461*, 1234−1242.

(4) Oosawa, F.; Kasai, M. A theory of linear and helical aggregations of macromolecules. *J. Mol. Biol.* **1962**, *4*, 10−21.

(5) Oosawa, F.; Asakura, S. *Thermodynamics of the Polymerization of Protein*; Academic Press, 1975.
(6) Kirschner, M.; Mitchison, T. Beyond self-assembly: From microtubules to morphogenesis. *Cell* **1986**, *45*, 329−342.
(7) Lüders, J.; Stearns, T. Microtubule-organizing centres: a re-evaluation. *Nat. Rev. Mol. Cell Biol.* **2007**, *8*, 161−167.
(8) Dominguez, R.; Holmes, K. C. Actin structure and function. *Annu. Rev. Biophys.* **2011**, *40*, 169−186.
(9) Kuriyan, J.; Eisenberg, D. The origin of protein interactions and allostery in colocalization. *Nature* **2007**, *450*, 983−990.
(10) Pawson, T.; Scott, J. D. Signaling Through Scaffold, Anchoring, and Adaptor Proteins. *Science* **1997**, *278*, 2075−2080.
(11) Mueller, A.; O'Brien, D. F. Supramolecular materials via polymerization of mesophases of hydrated amphiphiles. *Chem. Rev.* **2002**, *102*, 727−758.
(12) Ciferri, A. Supramolecular polymerizations. *Macromol. Rapid Commun.* **2002**, *23*, 511−529.
(13) Zhao, D.; Moore, J. S. Nucleation-elongation: A mechanism for cooperative supramolecular polymerization. *Org. Biomol. Chem.* **2003**, *1*, 3471−3491.
(14) Zhong, S.; Cui, H.; Chen, Z.; Wooley, K. L.; Pochan, D. J. Helix self-assembly through the coiling of cylindrical micelles. *Soft Matter* **2007**, *4*, 90−93.
(15) De Greef, T. F. A.; Smulders, M. M. J.; Wolffs, M.; Schenning, A. P. H. J.; Sijbesma, R. P.; Meijer, E. W. Supramolecular polymerization. *Chem. Rev.* **2009**, *109*, 5687−5754.
(16) Aida, T.; Meijer, E. W.; Stupp, S. I. Functional supramolecular polymers. *Science* **2012**, *335*, 813−817.
(17) Ogi, S.; Sugiyasu, K.; Manna, S.; Samitsu, S.; Takeuchi, M. Living supramolecular polymerization realized through a biomimetic approach. *Nat. Chem.* **2014**, *6*, 188−195.
(18) Kang, J.; Miyajima, D.; Mori, T.; Inoue, Y.; Itoh, Y.; Aida, T. A rational strategy for the realization of chain-growth supramolecular polymerization. *Science* **2015**, *347*, 646−651.
(19) Lutz, J.-F.; Lehn, J.-M.; Meijer, E. W.; Matyjaszewski, K. From precision polymers to complex materials and systems. *Nat. Rev. Mater.* **2016**, *1*, 16024.
(20) Sorrenti, A.; Leira-Iglesias, J.; Markvoort, A. J.; De Greef, T. F. A.; Hermans, T. M. Non-equilibrium supramolecular polymerization. *Chem. Soc. Rev.* **2017**, *46*, 5476−5490.
(21) Wehner, M.; Würthner, F. Supramolecular polymerization through kinetic pathway control and living chain growth. *Nat. Rev. Chem.* **2020**, *4*, 38−53.
(22) Hashim, P. K.; Bergueiro, J.; Meijer, E. W.; Aida, T. Supramolecular Polymerization: A Conceptual Expansion for Innovative Materials. *Prog. Polym. Sci.* **2020**, *105*, 101250.
(23) Baumgartner, R.; Fu, H.; Song, Z.; Lin, Y.; Cheng, J. Cooperative polymerization of α-helices induced by macromolecular architecture. *Nat. Chem.* **2017**, *9*, 614−622.
(24) Chen, C.; Fu, H.; Baumgartner, R.; Song, Z.; Lin, Y.; Cheng, J. Proximity-Induced Cooperative Polymerization in "Hinged" Helical Polypeptides. *J. Am. Chem. Soc.* **2019**, *141*, 8680−8683.
(25) Song, Z.; Fu, H.; Wang, J.; Hui, J.; Xue, T.; Pacheco, L. A.; Yan, H.; Baumgartner, R.; Wang, Z.; Xia, Y.; Wang, X.; Yin, L.; Chen, C.; Rodríguez-López, J.; Ferguson, A. L.; Lin, Y.; Cheng, J. Synthesis of polypeptides via bioinspired polymerization of in situ purified N-carboxyanhydrides. *Proc. Natl. Acad. Sci. U.S.A.* **2019**, *116*, 10658−10663.
(26) Song, Z.; Fu, H.; Baumgartner, R.; Zhu, L.; Shih, K.-C.; Xia, Y.; Zheng, X.; Yin, L.; Chipot, C.; Lin, Y.; Cheng, J. Enzyme-mimetic self-catalyzed polymerization of polypeptide helices. *Nat. Commun.* **2019**, *10*, 5470.
(27) Doty, P.; Lundberg, R. D. Polypeptides. X. Configurational and stereochemical effects in the amine-initiated polymerization of N-carboxyanhydrides. *J. Am. Chem. Soc.* **1956**, *78*, 4810−4812.
(28) Lundberg, R. D.; Doty, P. Polypeptides. XVII. A study of the kinetics of the primary amine-initiated polymerization of N-carboxy-anhydrides with special reference to configurational and stereo-chemical effects. *J. Am. Chem. Soc.* **1957**, *79*, 3961−3972.
(29) Ballard, D. G. H.; Bamford, C. H.; Elliott, A. Synthetic polypeptides. *Macromol. Chem. Phys.* **1960**, *35*, 222−238.
(30) Michaelis, L.; Menten, M. Die kinetik der invertinwirkung. *Biochem. J.* **1913**, *Z49*, 333−369.
(31) Dear, A. J.; Meisl, G.; Michaels, T. C. T.; Zimmermann, M. R.; Linse, S.; Knowles, T. P. J. The catalytic nature of protein aggregation. *J. Chem. Phys.* **2020**, *152*, 045101.
(32) Fersht, A. *Structure and Mechanism in Protein Science: A Guide to Enzyme Catalysis and Protein Folding*; Macmillan, 1999.
(33) Briggs, G. E.; Haldane, J. B. S. A Note on the Kinetics of Enzyme Action. *Biochem. J.* **1925**, *19*, 338−339.

https://doi.org/10.1021/acs.macromol.1c02606
Macromolecules 2022, 55, 2041−2050